HAL
open science

Rotational spectrum of ethyl cyanoacetylene (C2H5C≢C-C≢N), a compound of potential astrochemical interest

Sophie Carles, Harald Mollendal, Jean-Claude Guillemin

To cite this version:

Sophie Carles, Harald Mollendal, Jean-Claude Guillemin. Rotational spectrum of ethyl cyanoacetylene (C2H5C≢C-C≢N), a compound of potential astrochemical interest. Astronomy and Astrophysics - A&A, 2013, 558, pp.A6. 10.1051/0004-6361/201321427 . hal-00916559

HAL Id: hal-00916559

https://hal.science/hal-00916559v1

Submitted on 10 Dec 2013

HAL is a multi-disciplinary open access archive for the deposit and dissemination of scientific research documents, whether they are published or not. The documents may come from teaching and research institutions in France or abroad, or from public or private research centers.

L'archive ouverte pluridisciplinaire **HAL**, est destinée au dépôt et à la diffusion de documents scientifiques de niveau recherche, publiés ou non, émanant des établissements d'enseignement et de recherche français ou étrangers, des laboratoires publics ou privés.

A&A 558, A6 (2013)
DOI: 10.1051/0004-6361/201321427
© ESO 2013

Astronomy & Astrophysics

Rotational spectrum of ethyl cyanoacetylene ($C_2H_5C{\equiv}C{-}C{\equiv}N$), a compound of potential astrochemical interest

S. Carles[1,2], H. Møllendal[1], and J.-C. Guillemin[3]

[1] Centre for Theoretical and Computational Chemistry (CTCC), Department of Chemistry, University of Oslo, PO Box 1033 Blindern, 0315 Oslo, Norway
e-mail: sophie.carles@kjemi.uio.no
[2] Permanent address: Institut de Physique de Rennes, Département de Physique Moléculaire, UMR 6251 UR1-CNRS, Université de Rennes 1, Bâtiment 11 C, Campus de Beaulieu, 35042 Rennes Cedex, France
[3] Institut des Sciences Chimiques de Rennes, École Nationale Supérieure de Chimie de Rennes, CNRS, UMR 6226, 11 allée de Beaulieu CS 50837, 35708 Rennes Cedex 7, France

Received 7 March 2013 / Accepted 8 June 2013

ABSTRACT

Context. New radiotelescopes, such as the very sensitive ALMA, will enable the detection of interstellar molecules in much lower concentrations than previously possible. A successful identification of an interstellar molecule requires that laboratory microwave and millimeter-wave spectra are investigated. Several cyanopolyynes and alkynylcarbonitriles have already been detected in the interstellar medium (ISM). Cyanoacetylene ($HC{\equiv}C{-}C{\equiv}N$) is abundant in the ISM and its methyl derivative, 2-butynenitrile ($CH_3C{\equiv}C{-}C{\equiv}N$), is also present. The next derivative, ethyl cyanoacetylene, (2-pentynenitrile $C_2H_5C{\equiv}C{-}C{\equiv}N$) may also be present in interstellar space.
Aims. We report the rotational spectrum of the ethyl cyanoacetylene ($C_2H_5C{\equiv}C{-}C{\equiv}N$). This is hoped to facilitate identifying gaseous ethyl cyanoacetylene in the ISM.
Methods. We studied the rotational spectrum of $C_2H_5C{\equiv}C{-}C{\equiv}N$ between 13 and 116 GHz with the microwave spectrometer of the University of Oslo. The spectroscopic study was augmented by high-level quantum-chemical calculations at B3LYP/cc-pVTZ and CCSD/cc-pVTZ levels of theory.
Results. We present for the first time the rotational spectrum of the ethyl cyanoacetylene ($C_2H_5C{\equiv}C{-}C{\equiv}N$). We assigned 342 transitions of the vibrational ground state, accurate values were obtained for rotational and centrifugal distortion constants, and the dipole moment was determined as well.

Key words. methods: data analysis – surveys – molecular data – methods: analytical – techniques: spectroscopic

1. Introduction

About 180 molecules, ions, and radicals have been detected in the interstellar medium (ISM) and circumstellar shells. The vast majority of these species have been identified by means of their rotational spectra. As many as about 25 of these compounds contain the cyano group ($C{\equiv}N$). This group is not only found in neutral molecules, but also in radicals and ions in organic as well as inorganic compounds. Obviously, the cyano group is involved in a complex and comprehensive chemistry in the ISM. Organic compounds possessing the cyano group are usually called nitriles. Several series of nitriles exist in the ISM. One example is the $H(C{\equiv}C)_n{-}C{\equiv}N$ series, where members with n in the range 0 to 5 have been identified (Snyder & Buhl 1971; Turner 1971; Avery et al. 1976; Broten et al. 1976, 1978; Kroto et al. 1978; Little et al. 1978; Winnewisser & Walmsley 1978; Bell et al. 1997). Another similar series includes the methyl group (CH_3). Three examples of the $CH_3(C{\equiv}C)_n{-}C{\equiv}N$ series with $n = 0$–2 have been found (Solomon et al. 1971; Broten et al. 1984; Snyder et al. 2006). Two other nitriles of relevance for the studied compound, namely, $C_nH_{2n+1}C{\equiv}N$, where n is 2 or 3, exist in space (Johnson et al. 1977; Belloche et al. 2009). This first study of the rotational spectrum of ethyl cyanoacetylene ($C_2H_5C{\equiv}C{-}C{\equiv}N$) was performed because this nitrile is chemically closely related to members of these series of nitriles. This fact alone suggests that the studied compound may be a component of the ISM. Consequently, it was thought worthwhile to synthesize $C_2H_5C{\equiv}C{-}C{\equiv}N$ and study its rotational spectrum to obtain data for use in a potential detection of this compound anywhere in the ISM. It is not expected that $C_2H_5C{\equiv}C{-}C{\equiv}N$ is a prominent interstellar, cometary, or atmospheric specie, but, hopefully, new and vastly improved radio astronomical observatories such as ALMA may be capable of detecting it using the spectral material we present here. This paper is organized in several sections and a conclusion. Section 2 presents some possible chemical pathways for the formation of the studied compound. Section 3 gives some details about the experimental set-up and the ethyl cyanoacetylene synthesis. Section 4 covers the ab initio calculations and their analysis. Section 5 presents the experimental results and the assignment of the microwave spectrum. Section 6 is dedicated to the experimental dipole moment determination.

2. Possible formation mechanisms for ethyl cyanoacetylene

There are no experimental data for the heat of formation of ethyl cyanoacetylene, but it could be thermodynamically more stable than both $HC{\equiv}C{-}C{\equiv}N$ and $CH_3C{\equiv}C{-}C{\equiv}N$. There are two reasons for this assumption. First, the heat of formation decrease of the $C_nH_{2n+1}C{\equiv}N$ series with $n = 0$ to 3 is 135.14, 74.04, 51.46, and 31.2 kJ/mol. Secondly, in the analogous alkyne series $C_nH_{2n+1}C{\equiv}CH$ with $n = 0$ to 2, the

heat of formation decrease is 226.73, 185.4, and 165.2 kJ/mol (Nist web book accessed January 2013). Ethyl cyanoacetylene contains the saturated ethyl group (C_2H_5) and the unsaturated C≡C–C≡N part. The fact that several unsatured-satured molecules have been detected in the ISM including $C_2H_5C{\equiv}N$, n-$C_3H_7C{\equiv}N$, $C_2H_5OC(O)H$ (Belloche et al. 2009) and the following methyl species $CH_3C{\equiv}CC{\equiv}N$, $CH_3C{\equiv}CC{\equiv}CC{\equiv}N$, $CH_3C{\equiv}N$, $CH_3OC(O)H$, $CH_3C(O)NH_2$ (Brown et al. 1975; Churchwell & Winnewisser 1975; Hollis et al. 2006) makes it likely that ethyl cyanoacetylene may be also present in this medium.

The formation of complex molecules (six or more atoms) in dense interstellar clouds may be available in gas phase from precursors that are formed on the grain surface (Vasyunin & Herbst 2013). The radical-radical association and the radical-neutral reactions are known to be efficient at low temperature in the gas phase because they are generally energy-barierless (Troe 2003; Klippenstein et al. 2006). Considering these kind of reactions, we suggest several chemical pathways for the formation of ethyl cyanoacetylene.

Very recent high-level ab initio and density functional theory (DFT) calculations may indicate that $C_2H_5C{\equiv}C{-}C{\equiv}N$ and atomic hydrogen may be formed in a reaction between the precursor 1-butyne ($CH_3CH_2C{\equiv}CH$) and the C≡N radical (Jamal & Mebel 2013). The C≡N radical in the ISM has been observed for a long time (Solomon 1973; Allen & Knapp 1978) and has recently been proposed as tracer for the magnetic field characterization in several dense clouds (Hakobian & Crutcher 2011; Crutcher et al. 1999). It is worth noting that 1-butyne has so far not been identified in this medium, although it is listed as a potential interstellar compound (Woon & Herbst 2009) and its relative abundance upper limit compare to H_2 in TMC-1 has been estimated to 3×10^{-9} (Irvine 1987). This could be explained by a probably quite small abundance but also by a low dipole moment of only 0.76D (Landsberg & Suenram 1983).

A second chemical pathway for the formation of $C_2H_5C{\equiv}C{-}C{\equiv}N$ may be the gas phase radical-radical association reaction between C≡C–C≡N and the alkyl precursor C_2H_5. Only the C≡C–C≡N radical has been identified in the ISM to date (Guelin & Thaddeus 1977). C_2H_5 may be relatively abundant, but its small dipole moment (about 0.25 D (Rudic et al. 2004)) is not favorable for a potential detection. A third gas phase process with the same precursor may be the reaction between HC_3N and C_2H_5. This kind of addition-elimination has been studied in theory (James & Ogawa 1965; James & MacCallum 1965) and a few experimental studies in the laboratory have been made (Getty et al. 1967), but it could lead to a simple addition on the triple bond to form an alkenyl radical.

At last, an alternative answer could be the reaction of CH_3^+ cation and $CH_3C{\equiv}C{-}C{\equiv}N$ followed by a dissociative recombination of the generated cation $C_2H_5C{\equiv}C{-}C{\equiv}NH^+$ to form $C_2H_5C{\equiv}C{-}C{\equiv}N$ and H. CH_3^+ is probably a key compound in the carbon chemistry of the ISM and has been proposed as one of the most abundant positive ions in dense clouds in several works (Opendak & Varshalovich 1986). Several experimental works have been performed in the gas phase on similar reactions as CH_3^+ with CH_4, HC≡N, $CH_3C{\equiv}N$ or HC≡CC≡N (Anicich 2003). For all these reactions the exit channel that corresponds to the addition process has been observed.

All these reaction paths include some hypothetical (because not detected) precursor species, but remain possible. The fact that some detected compounds similar to ethyl cyanoacetylene, bearing a saturated ethyl group and an unsaturated group, have a smaller dipole moment therefore suggests a possible detection of $C_2H_5C{\equiv}C{-}C{\equiv}N$ if it is present in reasonable amounts.

3. Experimental

Ethyl cyanoacetylene (2-pentynenitrile) is usually synthesized by reaction of ClCN with 1-butynyl lithium (Van der Welle & Brandsma 1973; Brandsma & Verkruijsse 1981). ClCN is a very toxic compound, not easy to synthesize or use safely (Coleman et al. 1946). Consequently, we prepared ethyl cyanoacetylene by dehydratation of the corresponding amide in the same way as used by Moureu and Bongrand at the beginning of the 20th century to synthesize cyanoacetylene (Moureu & Bongrand 1920). Ethyl pent-2-ynoate was purchased from Alfa-Aesar and used without further purification. 2-Pentynamide was prepared as previously reported (Strubing et al. 2005).

In a 100 mL round-bottomed flask, 2-pentynamide (4.85 g, 50 mmol) was carefully mixed with sea sand (20 g) and phosphorus pentoxide (15 g). The flask was attached to a vacuum line equipped with two traps and evacuated. The flask was immersed in an oil bath, the first trap was immersed in a bath cooled at 0 °C and the second one in a bath cooled at −80 °C. The oil bath was gradually heated to 180 °C for about 2 h. High boiling impurities were trapped in the first trap and ethyl cyanoacetylene was selectively trapped in the second trap. At the end of the reaction, ethyl cyanoacetylene was transferred under vacuum to a cell equipped with a stopcock and the product was kept for months in a freezer (−20 °C) without any decomposition. Yield 72% (2.84 g, 3.6 mmol). ^{1}H and ^{13}C NMR data of 2-pentynamide and ethyl cyanoacetylene are as follows: 2-pentynamide: ^{1}H NMR ($CDCl_3$, 400 MHz, 25 °C) δ 1.16 (t, 3H, $^3J_{HH}$ = 7.5 Hz, CH_3) ; 2.28 (q, ^{2}H, $^3J_{HH}$ = 7.5 Hz, CH_2) ; 5.9 and 6.4 (s, brd, 2H, NH_2). ^{13}C NMR ($CDCl_3$, 100 MHz, 25 °C) δ 12.4 (q, $^1J_{CH}$ = 132.0 Hz, CH_3), 12.8 (t, $^1J_{CH}$ = 129.8 Hz, CH_2), 74.4 (s, $\underline{C}$-CO), 90.1 (s, $\underline{C}$C-CO), 155.7 (s, C=O). Ethyl cyanoacetylene: ^{1}H NMR ($CDCl_3$, 400 MHz, 25 °C) δ 1.22 (t, 3H, $^3J_{HH}$ = 7.5 Hz, CH_3); 2.36 (q, 2H, $^3J_{HH}$ = 7.5 Hz, CH_2). ^{13}C NMR ($CDCl_3$, 100 MHz, 25 °C) δ 11.9 (q, $^1J_{CH}$ = 132.3 Hz, CH_3), 12.6 (t, $^1J_{CH}$ = 129.8 Hz, CH_3), 54.6 (s, $\underline{C}$-CN), 88.4 (s, $\underline{C}$C-CN), 105.2 (s, CN).

The microwave spectrometer of the Oslo University used for this study has been described elsewhere (Møllendal et al. 2005, 2006). This spectrometer has a resolution of 0.5 MHz and measures the frequency of isolated transitions with an accuracy of 0.1 MHz. The frequency synthesizer is a 2–26.5 GHz 1730B Systron Donner model and the lock in amplifier control is a 0.5 Hz–120 kHz 5209 Perkin Elmer Instruments model. Several frequency multipliers were used to study the microwave spectrum of $C_2H_5C{\equiv}C{-}C{\equiv}N$ between 13–116 GHz spectral range by Stark modulation spectroscopy. Double-resonance radio-frequency microwave experiments (RFMWDR), similar to those performed by Wodarczyk and Wilson (Wodarczyk & Wilson 1971), were employed to unambiguously assign several transitions using the equipment described elsewhere (Leonov et al. 2000) The radio frequency source was a Rohde & Schwarz SML01 signal generator operating in the 9 kHz-1.1 GHz spectral region. An EIN Model 503L amplifier provided 3 W linear amplification of the radio signals between 2 and 510 MHz. Mixing of the radio signal with the Stark modulation signal was provided using a Hewlett-Packard 10514 mixer. The pressure in the spectrometer cell was approximately 10 Pa and the temperature was maintained at room temperature, or at −30 °C, by cooling the 2 m Hewlett-Packard absorption cell with dry ice to enhance intensities.

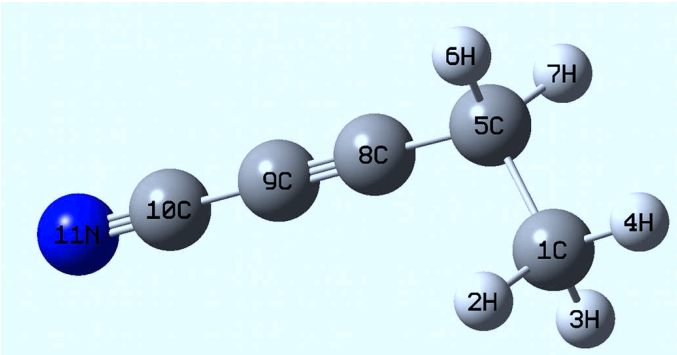

Fig. 1. Model of ethyl cyanoacetylene (2-pentynenitrile) with atom numbering.

4. Quantum-chemical calculations

Prediction of accurate spectroscopic constants greatly facilitates the assignment of complex rotational spectra such as that encountered for $CH_3CH_2C{\equiv}C{-}C{\equiv}N$. Fortunately, high-level quantum-chemical calculations are now capable of providing such parameters.

The present quantum-chemical calculations were performed employing the Gaussian 09 program package (Frisch et al. Gaussian09) running with the ABEL Linux cluster of the University of Oslo. Becke's three-parameter hybrid functional (Becke 1988) employing the Lee, Yang, and Parr correlation functional (B3LYP; Lee et al. 1988) was used in the density functional theory calculations (DFT). Ab initio coupled-cluster calculations with singlet and doublet excitations (CCSD; Purvis & Bartlett 1982; Scuseria et al. 1988) were also undertaken. Peterson and Dunning's correlation consistent cc-pVTZ basis set, (Peterson & Dunning 2002) which is of triple-ζ quality, was used in the calculations.

A model of ethyl cyanoacetylene with atom numbering is shown in Fig. 1. The geometry was first optimized at the B3LYP/cc-pVTZ level theory employing the default convergence criteria of Gaussian09. The molecule has C_S symmetry plane with four out-of-plane hydrogen atoms (H2, H3, H4, H6 and H7). The B3LYP structure is shown in Table 1. The B3LYP dipole moment and its components along the principal inertial axes, the vibrational frequencies, Watson's S-reduction quartic and sextic centrifugal distortion constants (Watson 1977), the vibration-rotation constants (the α's) (Gordy & Cook 1984), and the nuclear quadrupole coupling constants of the ^{14}N atom were then calculated. In these calculations, the B3LYP structure was held fixed in the principal inertial axis coordinate system to obtain correct centrifugal distortion and α-constants, as pointed out by McKean et al. (McKean et al. 2008). The dipole moment and the nuclear quadrupole coupling constants are listed in Table 2, the theoretical fundamental vibrational frequencies in Table 3, the α's in Table 4, and the centrifugal distortion constants in Table 5. Finally, the geometry was optimized at the very high CCSD/cc-pVTZ level of theory. The resulting structure is listed in Table 1. The dipole moment and the ^{14}N quadrupole coupling constants are given in Table 2. It was not possible to calculate vibrational properties at this level of theory with our present computational resources. Interestingly, the bond lengths (Table 1) are very similar at both theory levels except for two of them, namely, the C5-C8 and the C9-C10 bond lengths. These B3LYP bonds are shorter by 1.15 and 1.74 pm, respectively. The angles and dihedral angles agree well. The total dipole moments are μ_{TOT} = 5.41 D (B3LYP), and μ_{TOT} = 5.59 D (CCSD) (Table 2).

Table 1. Theoritical structures, principal moments of inertia, and rotational constants.

Method:	CCSD / cc-pVTZ	B3LYP / cc-pVTZ
	Bond lengths (pm)	
$C1-H2$	108.88	108.89
$C1-H3$	108.88	108.89
$C1-H4$	108.90	108.94
$C1-C5$	153.21	153.76
$C5-H6$	109.10	109.34
$C5-H7$	109.10	109.34
$C5-C8$	146.41	145.26
$C8\equiv C9$	120.66	120.55
$C9-C10$	138.34	136.60
$C10\equiv N11$	115.82	115.65
	Angles (degree)	
$H2-C1-H3$	108.27	108.23
$H2-C1-H4$	108.53	108.45
$H2-C1-C5$	110.74	110.90
$H3-C1-H4$	108.53	108.45
$H3-C1-C5$	110.74	110.90
$H4-C1-C5$	109.97	109.83
$C1-C5-H6$	110.39	110.04
$C1-C5-H7$	110.39	110.04
$C1-C5-C8$	112.23	113.14
$H6-C5-H7$	106.92	106.30
$H6-C5-C8$	108.36	108.54
$H7-C5-C8$	108.36	108.54
$C5-C8\equiv C9$	179.00	179.09
$C8\equiv C9-C10$	179.84	179.78
$C9-C10\equiv N11$	179.95	179.95
	Dihedral angles (degree)	
$H2-C1-C5-H6$	60.94	61.45
$H2-C1-C5-H7$	178.94	178.26
$H2-C1-C5-C8$	−60.06	−60.14
$H3-C1-C5-H6$	−178.94	−178.26
$H3-C1-C5-H7$	−60.94	−61.45
$H3-C1-C5-C8$	60.06	60.14
$H4-C1-C5-H6$	−59.00	−58.40
$H4-C1-C5-H7$	59.00	58.40
$H4-C1-C5-C8$	180.00	180.00
	Principal moments of inertia (amu Å^2)^a	
I_a	23.10	22.88
I_b	377.59	375.58
I_c	394.46	392.24
$I_c-I_a-I_b$	−6.24	−6.22
	Rotational constants (MHz)	
A	21878.3	22088.3
B	1338.4	1345.6
C	1281.2	1288.5

Notes. $^{(a)}$ Conversion factor is 505379.05 MHz amu Å^2.

5. Microwave spectrum and assignment

The CCSD calculations (Table 2) predict a large dipole moment for $C_2H_5C{\equiv}C{-}C{\equiv}N$ with a component of 5.55 D along the a-principal inertia axis, and a much smaller component of 0.69 D along the b-axis. The molecule is almost a completely prolate symmetrical top because of Ray's asymmetry parameter (Ray 1932) $\kappa \approx -0.994$. The spectrum was therefore predicted to be

Table 2. Theoritical dipole moments and quadrupole coupling constants.

Method:	CCSD/cc-pVTZ	B3LYP/cc-pVTZ
	Dipole moments (Debye)	
μ_a	5.55	5.37
μ_b	0.69	0.67
μ_C	0.00	0.00
μ_{TOT}	5.59	5.41
	^{14}N Quadrupole coupling constants (MHz)	
χ_{aa}	–4.22	–4.50
χ_{bb}	2.03	2.17
χ_{cc}	2.19	2.33
χ_{ab}	–1.07	–1.15

Table 3. Fundamental vibrational frequencies (cm^{-1}).

	Harmonic	Anharmonic
1(1)	3118.4	2979.0
2(1)	3114.5	2974.4
3(1)	3050.3	2901.1
4(1)	3046.0	2920.1
5(1)	3024.6	2942.4
6(1)	2391.4	2385.5
7(1)	2258.6	2226.0
8(1)	1506.9	1490.0
9(1)	1499.1	1478.1
10(1)	1470.8	1448.3
11(1)	1419.8	1380.7
12(1)	1351.1	1308.3
13(1)	1287.3	1246.4
14(1)	1171.5	1177.6
15(1)	1106.2	1080.1
16(1)	1077.6	1051.0
17(1)	954.0	929.3
18(1)	789.7	777.0
19(1)	670.3	659.4
20(1)	558.3	552.1
21(1)	544.3	539.2
22(1)	488.9	487.5
23(1)	375.4	365.3
24(1)	245.4	241.8
25(1)	233.0	212.2
26(1)	133.0	128.1
27(1)	103.3	96.3

Table 4. The B3LYP/cc-pVTZ vibro-rot alpha matrix (MHz).

	a	*b*	*c*
Q(1)	19.94	–0.09	–0.06
Q(2)	14.76	0.13	0.08
Q(3)	–31.47	0.57	0.38
Q(4)	26.30	0.01	0.00
Q(5)	–15.82	0.60	0.33
Q(6)	11.71	4.53	4.19
Q(7)	8.61	3.21	2.97
Q(8)	20.41	–0.12	–1.01
Q(9)	–208.68	–0.30	–0.12
Q(10)	–25.31	0.27	–0.56
Q(11)	239.76	0.19	0.88
Q(12)	121.84	–0.60	1.05
Q(13)	147.55	–1.06	–1.07
Q(14)	8.73	2.87	2.68
Q(15)	–302.76	0.87	0.51
Q(16)	457.09	–0.76	0.11
Q(17)	198.76	0.15	0.91
Q(18)	–15.50	0.97	0.92
Q(19)	37.96	0.47	0.87
Q(20)	–3670.71	–1.31	–0.58
Q(21)	3448.64	–0.75	–1.45
Q(22)	–238.99	1.46	1.11
Q(23)	206.87	–1.13	–1.35
Q(24)	–1359.71	–2.60	–1.73
Q(25)	1309.69	0.04	–0.20
Q(26)	–817.30	–1.32	–1.97
Q(27)	684.85	–3.19	–1.53

Table 5. B3LYP/cc-pVTZ centrifugal distortion constants.

Quartic Centrifugal Distortion Constants (MHz)			
(Asymmetrically reduced)		(Symmetrically reduced)	
Δ_J	0.000146	D_J	0.000143
Δ_K	0.972	D_K	0.972
Δ_{JK}	−0.0126	D_{JK}	−0.0126
δ_J	0.0000225	d_1	−0.0000225
δ_K	0.00381	d_2	−0.00000131
Sextic Centrifugal Distortion Constants (MHz)			
(Asymmetrically reduced)		(Symmetrically reduced)	
Φ_J	$0.14E-09$	H_J	$0.15E-09$
Φ_K	$-0.79E-03$	H_K	$-0.79E-03$
Φ_{JK}	$-0.13E-06$	H_{JK}	$-0.14E-06$
Φ_{KJ}	$0.14E-04$	H_{KJ}	$0.14E-04$
ϕ_J	$0.41E-10$	h_1	$0.40E-10$
ϕ_K	$0.25E-05$	h_2	$-0.61E-11$
ϕ_{JK}	$-0.26E-07$	h_3	$0.48E-12$

dominated by pile-ups of *a*-type *R*-branch transitions of ground- and vibrationally excited states separated by almost the exact sum of the B and C rotational constants.

The pile-ups were expected to have a very complex fine-structure, especially for high values of the *J* quantum number, because there are six transitions with fundamental frequencies below 500 cm^{-1} (Table 3) and each of the corresponding excited states will contribute their own spectra to each pile-up, making them very crowded. At low values of *J*, most of the K_{-1} lines will coalesce into one big, unresolved line, but at high values of *J*, centrifugal distortion will split the K_{-1} lines, allowing individual states to be assigned. This too adds to the complexity of the spectrum.

These predictions turned out to be true. For high values of *J*, a $J+1 \leftarrow J$ pile-up covers a spectral region of several hundred MHz. A portion of one such pile-up involving the $J = 33 \leftarrow 32$ transition, is shown in Fig. 2. Ground-state transitions overlapping with vibrationally excited state lines occur frequently and severely complicated the assignment of this spectrum. The first unambiguous assignments were achieved in RFMWDR experiments performed on pairs of lines with the same K_{-1} pseudo-quantum number using the theoretical rotational and centrifugal distortion constants to predict their approximate frequencies. The Stark effect was also useful for the assignments of several transitions. The assignments were then gradually extended to

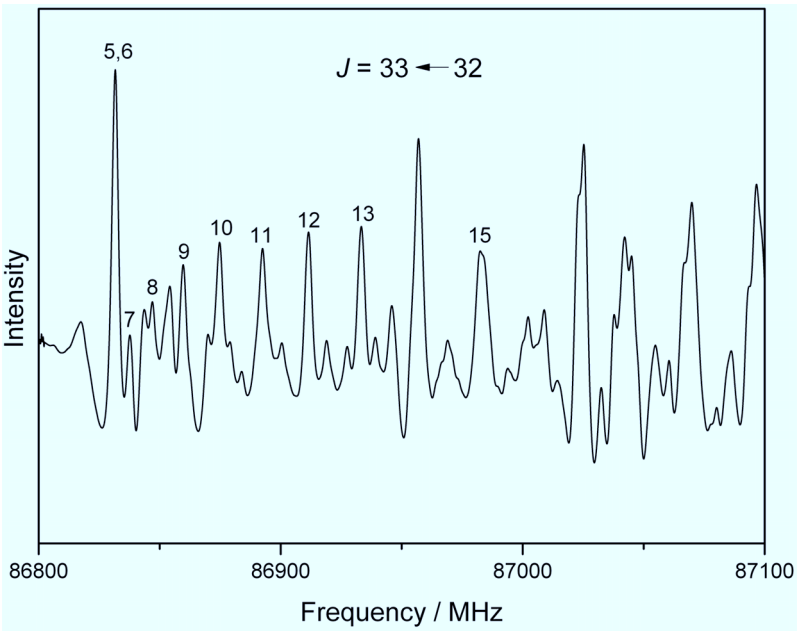

Fig. 2. Portion of the $J = 33 \leftarrow 32$ transition of the rotational spectrum of $C_2H_5C{\equiv}C{-}C{\equiv}N$ taken at a Stark field of about 150 V/cm. The values above several of the absorption peaks refer to the K_{-1} pseudo-quantum number. It was not possible to definitely assign values of K_{-1} higher than 15 because of overlapping transitions (extreme right of the picture). The most intense line to the extreme left consists of the unresolved $K_{-1} = 5$ and 6 transitions.

include more K_{-1}-transitions and transitions with increasingly higher values of J.

Sørensen's program ROTFIT (Sørensen 1967) was used for a least-squares fit of the lines employing Watson's S-reduction and Ir-representation (Watson 1977). Sharp and well-isolated transitions were assigned an uncertainty of 0.10 MHz, whereas larger uncertainties were used for other transitions. Because overlapping of transitions occurs very frequently, only well-isolated lines were included in the fit. Ultimately, 342 ^aR-transitions of the ground vibrational state (Table 6) were selected to obtain the best possible spectroscopic constants and a root-mean-square deviation (rms) similar to the experimental uncertainty of ±0.1 MHz. Values of the J quantum number between 3 and 44, and K_{-1} between 0 and 15 (Table 6) were employed. Comparatively few transitions with $K_{-1} = 0$, 1, and 2 were included in the fit because they frequently overlap with other transitions, or because they were not fully Stark-modulated and therefore could not be measured accurately. Attempts to assign b-type lines failed, presumably because μ_b is as small as 0.659(3) D (see below), producing insufficient intensities for secure assignments. It was not possible to derive the quadrupole coupling constants of ^{14}N, because the corresponding splittings of the ^aR-lines are small and not resolved. This is in accord with predictions from program MB09 (Marstokk & Møllendal 1969) using the theoretical nuclear quadrupole coupling constants shown in Table 2.

In the fitting of the ^aR-lines, only the rotational constants and the centrifugal distortion constants D_J, D_{JK}, H_J, H_{JK}, and D_{KJ} were employed, with the remaining centrifugal distortion constants preset at zero. This was done because the compound is practically a symmetrical top ($\kappa \approx -0.9942$; Table 6). The centrifugal distortion constants excluded from the fit will therefore play an insignificant role. The resulting spectroscopic constants are shown in Table 7. This table also includes their theoretical counterparts. Excellent agreement exists between the experimental and CCSD rotational constants. The experimental quartic centrifugal distortion constants are in satisfactory agreement with their B3LYP counterparts, whereas the sextic B3LYP centrifugal distortion constants disagree with their experimental equivalents. It is seen from this table that the A rotational constant is poorly determined. The reason for this is that only ^aR-lines were assigned for this very prolate compound. Nevertheless, the spectroscopic constants shown in this table should be able to predict the frequencies of ^aR-transitions in spectral regions not covered by us with a very high degree of precision, because the A rotational constant influences the predictions to a minor degree.

Attempts to assign excited states were also made. These attempts met with some success, but we did not obtain results that warrant publication because of the very crowded nature of the spectrum.

6. Dipole moment

The dipole moment was determined by a least-squares fitting of the second-order Stark coefficient shown in Table 8. The weight of each Stark coefficient was taken to be the inverse square of its standard deviation, which is also shown in the same table. The theoretical values of the second-order Stark coefficients were calculated as described by Golden and Wilson (Golden & Wilson 1948) using program MB04 (Marstokk & Møllendal 1969). The experimental dipole moment components are $\mu_a = 5.713(28)$, $\mu_b = 0.659(3)$, $\mu_c = 0.0$ (preset) and $\mu_{TOT} = 5.751(28)$ Debye, where the uncertainties are 1 standard deviation. The dipole moment along the c-principal inertial axis, μ_c, is exactly zero because $C_2H_5C{\equiv}C{-}C{\equiv}N$ has a symmetry plane. These experimental values agree well with the calculated dipole moments at the B3LYP/cc-pVTZ and CCSD/cc-pVTZ levels of theory (Table 2).

7. Conclusion

The microwave spectrum of the ground-vibrational state of ethyl cyanoacetylene was investigated in the 13–116 GHz range and 342 transitions with a maximum $J = 44$ and maximum $K_{-1} = 15$ were assigned and the experimental dipole moment was determined. The spectroscopic constants obtained from the least-squares fit should be capable of predicting very accurate frequencies of transitions that do not appear in the investigated spectral range. Hopefully, this spectral analysis of $C_2H_5C{\equiv}C{-}C{\equiv}N$ will allow its detection in the ISM provided it is present in a suitable concentration.

Table 6. Rotational spectrum of $C_2H_5C{\equiv}C{-}C{\equiv}N$.

Watson *S*-reduction											
Total number of transitions: 342											
Transition						Obs. frequency	Obs. – calc.	Weight	*t*	Distortion corrections	
										total	higher
3	1	3	4	1	4	10 402.26	–0.066	0.10	–0.6	0.068	–4.600E-6
4	1	4	5	1	5	13 002.79	0.153	0.10	1.3	0.056	–4.100E-6
4	1	3	5	1	4	13 299.18	–0.148	0.15	–0.9	0.056	–4.100E-6
5	1	5	6	1	6	15 602.66	–0.109	0.10	–0.9	0.024	–2.600E-7
5	1	4	6	1	5	15 958.99	0.197	0.20	0.8	0.024	–2.600E-7
6	1	6	7	1	7	18 202.68	–0.006	0.10	–0.1	–0.032	9.900E-6
6	1	5	7	1	6	18 617.99	–0.047	0.10	–0.4	–0.032	9.900E-6
7	1	7	8	1	8	20 802.25	–0.105	0.10	–0.9	–0.114	3.100E-5
8	0	8	9	0	9	23 656.73	0.013	0.10	0.1	–0.474	1.000E-4
8	1	8	9	1	9	23 401.56	–0.182	0.10	–1.6	–0.228	6.700E-5
8	1	7	9	1	8	23 935.70	–0.012	0.10	–0.1	–0.228	6.700E-5
9	0	9	10	0	10	26 281.13	0.093	0.10	0.8	–0.649	1.700E-4
9	1	9	10	1	10	26 000.45	–0.363	0.15	–2.1	–0.377	1.300E-4
9	1	8	10	1	9	26 593.98	–0.084	0.10	–0.8	–0.377	1.300E-4
9	7	3	10	7	4	26 316.27	–0.124	0.15	–0.7	12.744	–0.027
9	7	2	10	7	3	26 316.27	–0.124	0.15	–0.7	12.744	–0.027
10	0	10	11	0	11	28 904.04	0.003	0.10	0.0	–0.863	2.800E-4
10	1	10	11	1	11	28 599.62	0.083	0.10	0.8	–0.565	2.200E-4
10	1	9	11	1	10	29 252.17	0.131	0.10	1.2	–0.565	2.200E-4
10	7	4	11	7	5	28 947.95	–0.036	0.15	–0.2	13.868	–0.030
10	7	3	11	7	4	28 947.95	–0.036	0.15	–0.2	13.868	–0.030
11	0	11	12	0	12	31 525.58	–0.010	0.10	–0.1	–1.120	4.300E-4
11	1	11	12	1	12	31 197.97	0.089	0.10	0.8	–0.795	3.600E-4
11	1	10	12	1	11	31 909.87	0.273	0.15	1.6	–0.795	3.600E-4
11	2	10	12	2	11	31 557.96	0.003	0.10	0.0	0.190	–1.200E-5
11	6	6	12	6	7	31 575.78	0.186	0.15	1.1	10.690	–0.018
11	6	5	12	6	6	31 575.78	0.186	0.15	1.1	10.690	–0.018
11	7	5	12	7	6	31 579.52	–0.044	0.15	–0.3	14.949	–0.033
11	7	4	12	7	5	31 579.52	–0.044	0.15	–0.3	14.949	–0.033
11	8	4	12	8	5	31 584.15	–0.138	0.15	–0.8	19.857	–0.055
11	8	3	12	8	4	31 584.15	–0.138	0.15	–0.8	19.857	–0.055
11	9	3	12	9	4	31 589.76	0.041	0.15	0.2	25.413	–0.087
11	9	2	12	9	3	31 589.76	0.041	0.15	0.2	25.413	–0.087
12	0	12	13	0	13	34 145.42	–0.152	0.10	–1.5	–1.423	6.400E-4
12	1	12	13	1	13	33 795.93	0.114	0.10	1.1	–1.073	5.500E-4
12	1	11	13	1	12	34 566.91	0.215	0.15	1.3	–1.073	5.500E-4
12	2	11	13	2	12	34 186.42	0.011	0.10	0.1	–0.005	1.200E-4
12	6	7	13	6	8	34 206.88	–0.001	0.10	0.0	11.369	–0.020
12	6	6	13	6	7	34 206.88	–0.001	0.10	0.0	11.369	–0.020
12	7	6	13	7	7	34 211.02	–0.108	0.15	–0.6	15.982	–0.036
12	7	5	13	7	6	34 211.02	–0.108	0.15	–0.6	15.982	–0.036
12	8	5	13	8	6	34 216.13	–0.081	0.15	–0.5	21.300	–0.060
12	8	4	13	8	5	34 216.13	–0.081	0.15	–0.5	21.300	–0.060
12	9	4	13	9	5	34 222.06	–0.010	0.10	–0.1	27.318	–0.095
12	9	3	13	9	4	34 222.06	–0.010	0.10	–0.1	27.318	–0.095
13	0	13	14	0	14	36 763.68	–0.182	0.15	–1.1	–1.775	9.200E-4
13	1	13	14	1	14	36 393.55	0.238	0.10	2.3	–1.401	8.200E-4
13	1	12	14	1	13	37 223.53	0.239	0.15	1.4	–1.400	8.200E-4
13	2	12	14	2	13	36 814.42	–0.111	0.10	–1.0	–0.251	3.100E-4
13	6	8	14	6	9	36 838.09	–0.076	0.15	–0.4	11.997	–0.022
13	6	7	14	6	8	36 838.09	–0.076	0.15	–0.4	11.997	–0.022
13	7	7	14	7	8	36 842.46	–0.217	0.10	–1.9	16.965	–0.039
13	7	6	14	7	7	36 842.46	–0.217	0.10	–1.9	16.965	–0.039
13	8	6	14	8	7	36 847.90	–0.210	0.15	–1.2	22.691	–0.066
13	8	5	14	8	6	36 847.90	–0.210	0.15	–1.2	22.691	–0.066
13	9	5	14	9	6	36 854.33	–0.062	0.15	–0.4	29.173	–0.104
13	9	4	14	9	5	36 854.33	–0.062	0.15	–0.4	29.173	–0.104
14	0	14	15	0	15	39 380.28	–0.065	0.15	–0.4	–2.181	1.300E-3
14	1	14	15	1	15	38 990.61	0.269	0.15	1.6	–1.783	1.200E-3
14	2	13	15	2	14	39 442.21	–0.087	0.10	–0.8	–0.552	5.900E-4
14	6	9	15	6	10	39 469.32	–0.127	0.15	–0.7	12.570	–0.023
14	6	8	15	6	9	39 469.32	–0.127	0.15	–0.7	12.570	–0.023

Table 6. continued.

Watson *S*-reduction											
Total number of transitions: 342											
Transition						Obs. frequency	Obs. – calc.	Weight	*t*	Distortion corrections	
										total	higher
14	7	8	15	7	9	39 474.39	0.182	0.15	1.0	17.893	–0.042
14	7	7	15	7	8	39 474.39	0.182	0.15	1.0	17.893	–0.042
14	8	7	15	8	8	39 479.91	–0.072	0.15	–0.4	24.028	–0.071
14	8	6	15	8	7	39 479.91	–0.072	0.15	–0.4	24.028	–0.071
14	9	6	15	9	7	39 486.68	–0.001	0.10	0.0	30.972	–0.112
14	9	5	15	9	6	39 486.68	–0.001	0.10	0.0	30.972	–0.112
14	10	5	15	10	6	39 494.17	–0.088	0.15	–0.5	38.723	–0.169
14	10	4	15	10	5	39 494.17	–0.088	0.15	–0.5	38.723	–0.169
14	11	4	15	11	5	39 502.86	0.178	0.15	1.0	47.276	–0.244
14	11	3	15	11	4	39 502.86	0.178	0.15	1.0	47.276	–0.244
16	3	14	17	3	15	44 728.52	–0.125	0.15	–0.7	0.987	–5.300E-4
16	3	13	17	3	14	44 730.79	0.104	0.15	0.6	0.985	–5.300E-4
16	7	10	17	7	11	44 737.32	0.106	0.10	0.9	19.568	–0.049
16	7	9	17	7	10	44 737.32	0.106	0.10	0.9	19.568	–0.049
16	8	9	17	8	10	44 743.46	–0.181	0.15	–1.0	26.521	–0.082
16	8	8	17	8	9	44 743.46	–0.181	0.15	–1.0	26.521	–0.082
16	9	8	17	9	9	44 751.25	0.096	0.10	0.8	34.391	–0.129
16	9	7	17	9	8	44 751.25	0.096	0.10	0.8	34.391	–0.129
16	11	6	17	11	7	44 769.13	–0.059	0.10	–0.5	52.867	–0.281
16	11	5	17	11	6	44 769.13	–0.059	0.10	–0.5	52.867	–0.281
17	7	11	18	7	12	47 368.58	–0.106	0.10	–0.9	20.308	–0.052
17	7	10	18	7	11	47 368.58	–0.106	0.10	–0.9	20.308	–0.052
17	11	7	18	11	8	47 402.40	0.028	0.15	0.2	55.564	–0.299
17	11	6	18	11	7	47 402.40	0.028	0.15	0.2	55.564	–0.299
18	3	16	19	3	17	49 992.91	–0.087	0.15	–0.5	0.211	5.200E-4
18	3	15	19	3	16	49 996.66	0.094	0.15	0.5	0.208	5.200E-4
18	8	11	19	8	12	50 007.12	–0.054	0.10	–0.5	28.748	–0.093
18	8	10	19	8	11	50 007.12	–0.054	0.10	–0.5	28.748	–0.093
18	9	10	19	9	11	50 015.44	–0.030	0.10	–0.3	37.543	–0.146
18	9	9	19	9	10	50 015.44	–0.030	0.10	–0.3	37.543	–0.146
18	10	9	19	10	10	50 025.11	0.178	0.10	1.5	47.359	–0.220
18	10	8	19	10	9	50 025.11	0.178	0.10	1.5	47.359	–0.220
18	11	8	19	11	9	50 035.49	–0.013	0.10	–0.1	58.191	–0.318
18	11	7	19	11	8	50 035.49	–0.013	0.10	–0.1	58.191	–0.318
19	3	17	20	3	18	52 625.38	0.002	0.15	0.0	–0.287	1.300E-3
19	3	16	20	3	17	52 630.09	0.095	0.15	0.6	–0.290	1.300E-3
19	7	13	20	7	14	52 631.64	0.076	0.15	0.4	21.574	–0.059
19	7	12	20	7	13	52 631.64	0.076	0.15	0.4	21.574	–0.059
19	9	11	20	9	12	52 647.26	–0.304	0.10	–2.6	39.009	–0.155
19	9	10	20	9	11	52 647.26	–0.304	0.10	–2.6	39.009	–0.155
20	3	18	21	3	19	55 258.03	0.138	0.15	0.8	–0.863	2.400E-3
20	3	17	21	3	18	55 263.97	0.183	0.15	1.1	–0.867	2.400E-3
20	4	17	21	4	18	55 253.26	0.109	0.15	0.6	3.161	–3.700E-3
20	4	16	21	4	17	55 253.26	0.040	0.15	0.2	3.161	–3.700E-3
20	5	16	21	5	17	55 253.26	–0.103	0.15	–0.6	8.330	–0.015
20	5	15	21	5	16	55 253.26	–0.103	0.15	–0.6	8.330	–0.015
20	6	15	21	6	16	55 257.34	0.279	0.10	2.4	14.640	–0.033
20	6	14	21	6	15	55 257.34	0.279	0.10	2.4	14.640	–0.033
20	8	13	21	8	14	55 270.66	0.095	0.10	0.8	30.678	–0.104
20	8	12	21	8	13	55 270.66	0.095	0.10	0.8	30.678	–0.104
20	9	12	21	9	13	55 279.77	0.158	0.10	1.4	40.398	–0.164
20	9	11	21	9	12	55 279.77	0.158	0.10	1.4	40.398	–0.164
20	10	11	21	10	12	55 290.07	0.089	0.10	0.8	51.246	–0.246
20	10	10	21	10	11	55 290.07	0.089	0.10	0.8	51.246	–0.246
20	11	10	21	11	11	55 301.56	–0.040	0.10	–0.3	63.217	–0.356
20	11	9	21	11	10	55 301.56	–0.040	0.10	–0.3	63.217	–0.356
20	12	9	21	12	10	55 314.39	–0.031	0.10	–0.3	76.305	–0.498
20	12	8	21	12	9	55 314.39	–0.031	0.10	–0.3	76.305	–0.498
21	6	16	22	6	17	57 888.54	0.225	0.15	1.3	14.721	–0.034
21	6	15	22	6	16	57 888.54	0.225	0.15	1.3	14.721	–0.034
21	8	14	22	8	15	57 902.12	–0.083	0.10	–0.7	31.521	–0.110
21	8	13	22	8	14	57 902.12	–0.083	0.10	–0.7	31.521	–0.110
21	9	13	22	9	14	57 911.60	–0.011	0.10	–0.1	41.704	–0.173

Table 6. continued.

Watson *S*-reduction											
Total number of transitions: 342											
Transition						Obs. frequency	Obs. – calc.	Weight	*t*	Distortion corrections	
										total	higher
21	9	12	22	9	13	57 911.60	–0.011	0.10	–0.1	41.704	–0.173
21	10	12	22	10	13	57 922.62	0.195	0.10	1.7	53.068	–0.260
21	10	11	22	10	12	57 922.62	0.195	0.10	1.7	53.068	–0.260
21	11	11	22	11	12	57 934.38	–0.180	0.10	–1.6	65.608	–0.375
21	11	10	22	11	11	57 934.38	–0.180	0.10	–1.6	65.608	–0.375
22	7	16	23	7	17	60 525.65	–0.046	0.10	–0.4	22.875	–0.068
22	7	15	23	7	16	60 525.65	–0.046	0.10	–0.4	22.875	–0.068
22	9	14	23	9	15	60 543.54	–0.020	0.10	–0.2	42.924	–0.182
22	9	13	23	9	14	60 543.54	–0.020	0.10	–0.2	42.924	–0.182
22	10	13	23	10	14	60 554.84	0.029	0.10	0.2	54.803	–0.273
22	10	12	23	10	13	60 554.84	0.029	0.10	0.2	54.803	–0.273
22	11	12	23	11	13	60 567.51	0.052	0.10	0.4	67.913	–0.395
22	11	11	23	11	12	60 567.51	0.052	0.10	0.4	67.913	–0.395
23	7	17	24	7	18	63 156.84	–0.179	0.10	–1.5	23.134	–0.070
23	7	16	24	7	17	63 156.84	–0.179	0.10	–1.5	23.134	–0.070
23	8	16	24	8	17	63 165.52	0.166	0.10	1.4	32.947	–0.120
23	8	15	24	8	16	63 165.52	0.166	0.10	1.4	32.947	–0.120
23	9	15	24	9	16	63 175.52	0.064	0.10	0.5	44.054	–0.191
23	9	14	24	9	15	63 175.52	0.064	0.10	0.5	44.054	–0.191
23	10	14	24	10	15	63 187.26	0.122	0.10	1.1	56.449	–0.287
23	10	13	24	10	14	63 187.26	0.122	0.10	1.1	56.449	–0.287
23	11	13	24	11	14	63 200.25	–0.041	0.10	–0.4	70.128	–0.415
23	11	12	24	11	13	63 200.25	–0.041	0.10	–0.4	70.128	–0.415
23	12	12	24	12	13	63 214.97	0.122	0.10	1.1	85.085	–0.580
23	12	11	24	12	12	63 214.97	0.122	0.10	1.1	85.085	–0.580
24	7	18	25	7	19	65 788.42	0.107	0.10	0.9	23.300	–0.073
24	7	17	25	7	18	65 788.42	0.107	0.10	0.9	23.300	–0.073
24	8	17	25	8	18	65 796.73	–0.134	0.10	–1.2	33.521	–0.126
24	8	16	25	8	17	65 796.73	–0.134	0.10	–1.2	33.521	–0.126
24	9	16	25	9	17	65 807.46	0.162	0.15	0.9	45.090	–0.200
24	9	15	25	9	16	65 807.46	0.162	0.15	0.9	45.090	–0.200
24	10	15	25	10	16	65 819.58	0.178	0.10	1.5	58.001	–0.301
24	10	14	25	10	15	65 819.58	0.178	0.10	1.5	58.001	–0.301
24	11	14	25	11	15	65 833.07	0.015	0.10	0.1	72.249	–0.434
24	11	13	25	11	14	65 833.07	0.015	0.10	0.1	72.249	–0.434
24	12	13	25	12	14	65 848.11	–0.072	0.10	–0.6	87.828	–0.607
24	12	12	25	12	13	65 848.11	–0.072	0.10	–0.6	87.828	–0.607
24	15	10	25	15	11	65 901.96	–0.012	0.10	–0.1	142.468	–1.439
24	15	9	25	15	10	65 901.96	–0.012	0.10	–0.1	142.468	–1.439
25	5	21	26	5	22	68 410.36	–0.071	0.15	–0.4	6.333	–0.012
25	5	20	26	5	21	68 410.36	–0.074	0.15	–0.4	6.333	–0.012
25	7	19	26	7	20	68 419.62	0.043	0.10	0.4	23.368	–0.075
25	7	18	26	7	19	68 419.62	0.043	0.10	0.4	23.368	–0.075
25	8	18	26	8	19	68 428.41	0.082	0.10	0.7	33.997	–0.131
25	8	17	26	8	18	68 428.41	0.082	0.10	0.7	33.997	–0.131
25	10	16	26	10	17	68 451.72	0.120	0.10	1.0	59.455	–0.314
25	10	15	26	10	16	68 451.72	0.120	0.10	1.0	59.455	–0.314
25	11	15	26	11	16	68 465.72	–0.028	0.15	–0.2	74.273	–0.454
25	11	14	26	11	15	68 465.72	–0.028	0.15	–0.2	74.273	–0.454
25	12	14	26	12	15	68 481.44	–0.002	0.10	0.0	90.473	–0.635
25	12	13	26	12	14	68 481.44	–0.002	0.10	0.0	90.473	–0.635
26	5	22	27	5	23	71 042.03	0.076	0.15	0.4	5.644	–0.010
26	5	21	27	5	22	71 042.03	0.072	0.15	0.4	5.644	–0.010
26	6	21	27	6	22	71 044.76	0.247	0.15	1.4	13.758	–0.037
26	6	20	27	6	21	71 044.76	0.247	0.15	1.4	13.758	–0.037
26	7	20	27	7	21	71 050.72	–0.089	0.10	–0.8	23.335	–0.077
26	7	19	27	7	20	71 050.72	–0.089	0.10	–0.8	23.335	–0.077
26	8	19	27	8	20	71 059.52	–0.223	0.10	–1.9	34.372	–0.135
26	8	18	27	8	19	71 059.52	–0.223	0.10	–1.9	34.372	–0.135
26	9	18	27	9	19	71 070.88	0.074	0.10	0.6	46.865	–0.217
26	9	17	27	9	18	71 070.88	0.074	0.10	0.6	46.865	–0.217
26	11	16	27	11	17	71 098.55	0.182	0.10	1.6	76.194	–0.474
26	11	15	27	11	16	71 098.55	0.182	0.10	1.6	76.194	–0.474

Table 6. continued.

Watson *S*-reduction											
Total number of transitions: 342											
Transition						Obs. frequency	Obs. – calc.	Weight	*t*	Distortion corrections	
										total	higher
26	12	15	27	12	16	71 114.43	–0.193	0.10	–1.7	93.017	–0.663
26	12	14	27	12	15	71 114.43	–0.193	0.10	–1.7	93.017	–0.663
27	7	21	28	7	22	73 681.91	–0.099	0.10	–0.9	23.196	–0.078
27	7	20	28	7	21	73 681.91	–0.099	0.10	–0.9	23.196	–0.078
27	8	20	28	8	21	73 690.90	–0.208	0.10	–1.8	34.642	–0.140
27	8	19	28	8	20	73 690.90	–0.208	0.10	–1.8	34.642	–0.140
27	9	19	28	9	20	73 702.39	–0.078	0.10	–0.7	47.597	–0.225
27	9	18	28	9	19	73 702.39	–0.078	0.10	–0.7	47.597	–0.225
27	11	17	28	11	18	73 731.16	0.249	0.10	2.1	78.010	–0.494
27	11	16	28	11	17	73 731.16	0.249	0.10	2.1	78.010	–0.494
27	12	16	28	12	17	73 747.51	–0.212	0.10	–1.8	95.455	–0.692
27	12	15	28	12	16	73 747.51	–0.212	0.10	–1.8	95.455	–0.692
28	9	20	29	9	21	76 333.99	–0.077	0.15	–0.4	48.219	–0.233
28	9	19	29	9	20	76 333.99	–0.077	0.15	–0.4	48.219	–0.233
29	9	21	30	9	22	78 965.56	–0.039	0.15	–0.2	48.728	–0.241
29	9	20	30	9	21	78 965.56	–0.039	0.15	–0.2	48.728	–0.241
29	10	20	30	10	21	78 979.96	0.267	0.15	1.5	64.217	–0.367
29	10	19	30	10	20	78 979.96	0.267	0.15	1.5	64.217	–0.367
29	11	19	30	11	20	78 995.91	0.153	0.15	0.9	81.310	–0.534
29	11	18	30	11	19	78 995.91	0.153	0.15	0.9	81.310	–0.534
29	12	18	30	12	19	79 013.64	–0.026	0.15	–0.1	99.998	–0.748
29	12	17	30	12	18	79 013.64	–0.026	0.15	–0.1	99.998	–0.748
30	9	22	31	9	23	81 597.12	0.057	0.10	0.5	49.120	–0.248
30	9	21	31	9	22	81 597.12	0.057	0.10	0.5	49.120	–0.248
30	12	19	31	12	20	81 646.33	–0.173	0.10	–1.5	102.095	–0.776
30	12	18	31	12	19	81 646.33	–0.173	0.10	–1.5	102.095	–0.776
30	13	18	31	13	19	81 666.77	–0.015	0.10	–0.1	123.044	–1.058
30	13	17	31	13	18	81 666.77	–0.015	0.10	–0.1	123.044	–1.058
31	9	23	32	9	24	84 228.35	–0.106	0.10	–0.9	49.392	–0.255
31	9	22	32	9	23	84 228.35	–0.106	0.10	–0.9	49.392	–0.255
31	10	22	32	10	23	84 243.38	0.098	0.15	0.6	65.911	–0.392
31	10	21	32	10	22	84 243.38	0.098	0.15	0.6	65.911	–0.392
31	12	20	32	12	21	84 279.20	–0.048	0.15	–0.3	104.071	–0.804
31	12	19	32	12	20	84 279.20	–0.048	0.15	–0.3	104.071	–0.804
31	13	19	32	13	20	84 300.12	–0.017	0.10	–0.1	125.694	–1.097
31	13	18	32	13	19	84 300.12	–0.017	0.10	–0.1	125.694	–1.097
32	8	25	33	8	26	86 846.94	–0.183	0.15	–1.1	34.274	–0.154
32	8	24	33	8	25	86 846.94	–0.183	0.15	–1.1	34.274	–0.154
32	9	24	33	9	25	86 859.70	–0.076	0.15	–0.4	49.538	–0.261
32	9	23	33	9	24	86 859.70	–0.076	0.15	–0.4	49.538	–0.261
32	10	23	33	10	24	86 874.75	–0.203	0.10	–1.8	66.573	–0.404
32	10	22	33	10	23	86 874.75	–0.203	0.10	–1.8	66.573	–0.404
32	13	20	33	13	21	86 933.30	–0.088	0.10	–0.8	128.220	–1.136
32	13	19	33	13	20	86 933.30	–0.088	0.10	–0.8	128.220	–1.136
33	7	27	34	7	28	89 468.20	–0.258	0.15	–1.5	19.937	–0.074
33	7	26	34	7	27	89 468.20	–0.258	0.15	–1.5	19.937	–0.074
33	9	25	34	9	26	89 490.72	–0.300	0.15	–1.7	49.556	–0.267
33	9	24	34	9	25	89 490.72	–0.300	0.15	–1.7	49.556	–0.267
34	4	31	35	4	32	92 108.79	–0.321	0.15	–1.9	–12.608	0.057
34	4	30	35	4	31	92 111.61	0.020	0.15	0.1	–12.615	0.057
35	10	26	36	10	27	94 769.52	0.076	0.15	0.4	67.771	–0.436
35	10	25	36	10	26	94 769.52	0.076	0.15	0.4	67.771	–0.436
35	11	25	36	11	26	94 788.13	–0.039	0.10	–0.3	88.273	–0.646
35	11	24	36	11	25	94 788.13	–0.039	0.10	–0.3	88.273	–0.646
35	12	24	36	12	25	94 809.22	–0.017	0.10	–0.1	110.688	–0.914
35	12	23	36	12	24	94 809.22	–0.017	0.10	–0.1	110.688	–0.914
35	13	23	36	13	24	94 832.38	–0.129	0.10	–1.1	135.006	–1.252
35	13	22	36	13	23	94 832.38	–0.129	0.10	–1.1	135.006	–1.252
36	10	27	37	10	28	97 400.66	–0.098	0.10	–0.8	67.895	–0.445
36	10	26	37	10	27	97 400.66	–0.098	0.10	–0.8	67.895	–0.445
36	11	26	37	11	27	97 419.99	0.092	0.10	0.8	88.965	–0.663
36	11	25	37	11	26	97 419.99	0.092	0.10	0.8	88.965	–0.663
36	12	25	37	12	26	97 441.65	0.178	0.10	1.5	112.001	–0.941

Table 6. continued.

Watson *S*-reduction											
Total number of transitions: 342											
Transition						Obs. frequency	Obs. – calc.	Weight	*t*	Distortion corrections	
										total	higher
36	12	24	37	12	25	97 441.65	0.178	0.10	1.5	112.001	–0.941
36	13	24	37	13	25	97 465.23	–0.098	0.10	–0.8	136.992	–1.290
36	13	23	37	13	24	97 465.23	–0.098	0.10	–0.8	136.992	–1.290
37	8	30	38	8	31	100 001.72	0.099	0.10	0.9	30.696	–0.149
37	8	29	38	8	30	100 001.72	0.099	0.10	0.9	30.696	–0.149
37	9	29	38	9	30	100 015.12	–0.084	0.15	–0.5	48.267	–0.279
37	9	28	38	9	29	100 015.12	–0.084	0.15	–0.5	48.267	–0.279
37	10	28	38	10	29	100 032.08	0.104	0.10	0.9	67.876	–0.453
37	10	27	38	10	28	100 032.08	0.104	0.10	0.9	67.876	–0.453
37	11	27	38	11	28	100 051.48	–0.044	0.10	–0.4	89.513	–0.679
37	11	26	38	11	27	100 051.48	–0.044	0.10	–0.4	89.513	–0.679
37	12	26	38	12	27	100 073.67	0.074	0.10	0.6	113.170	–0.967
37	12	25	38	12	26	100 073.67	0.074	0.10	0.6	113.170	–0.967
37	13	25	38	13	26	100 098.28	0.249	0.10	2.2	138.834	–1.327
37	13	24	38	13	25	100 098.28	0.249	0.10	2.2	138.834	–1.327
38	6	33	39	6	34	102 618.67	–0.128	0.10	–1.1	–0.213	0.029
38	6	32	39	6	33	102 618.67	–0.130	0.10	–1.2	–0.213	0.029
38	8	31	39	8	32	102 632.36	0.041	0.10	0.4	29.553	–0.144
38	8	30	39	8	31	102 632.36	0.041	0.10	0.4	29.553	–0.144
38	9	30	39	9	31	102 645.97	–0.070	0.15	–0.4	47.586	–0.280
38	9	29	39	9	30	102 645.97	–0.070	0.15	–0.4	47.586	–0.280
38	10	29	39	10	30	102 663.03	–0.067	0.10	–0.6	67.709	–0.460
38	10	28	39	10	29	102 663.03	–0.067	0.10	–0.6	67.709	–0.460
38	11	28	39	11	29	102 683.23	0.187	0.10	1.6	89.914	–0.694
38	11	27	39	11	28	102 683.23	0.187	0.10	1.6	89.914	–0.694
38	12	27	39	12	28	102 705.62	0.013	0.10	0.1	114.190	–0.991
38	12	26	39	12	27	102 705.62	0.013	0.10	0.1	114.190	–0.991
38	13	26	39	13	27	102 730.60	–0.015	0.10	–0.1	140.528	–1.364
38	13	25	39	13	26	102 730.60	–0.015	0.10	–0.1	140.528	–1.364
39	6	34	40	6	35	105 249.86	–0.086	0.10	–0.8	–2.270	0.042
39	6	33	40	6	34	105 249.86	–0.088	0.10	–0.8	–2.270	0.042
39	8	32	40	8	33	105 263.05	0.104	0.10	0.9	28.259	–0.137
39	8	31	40	8	32	105 263.05	0.104	0.10	0.9	28.259	–0.137
39	10	30	40	10	31	105 293.84	–0.277	0.15	–1.6	67.390	–0.466
39	10	29	40	10	30	105 293.84	–0.277	0.15	–1.6	67.390	–0.466
39	11	29	40	11	30	105 314.51	0.058	0.10	0.5	90.162	–0.708
39	11	28	40	11	29	105 314.51	0.058	0.10	0.5	90.162	–0.708
39	12	28	40	12	29	105 337.63	0.129	0.10	1.1	115.060	–1.016
39	12	27	40	12	28	105 337.63	0.129	0.10	1.1	115.060	–1.016
39	15	25	40	15	26	105 421.31	–0.026	0.10	–0.2	202.380	–2.455
39	15	24	40	15	25	105 421.31	–0.026	0.10	–0.2	202.380	–2.455
40	6	35	41	6	36	107 881.30	0.212	0.20	0.9	–4.483	0.058
40	6	34	41	6	35	107 881.30	0.210	0.20	0.9	–4.483	0.058
40	8	33	41	8	34	107 893.67	0.170	0.10	1.5	26.810	–0.129
40	8	32	41	8	33	107 893.67	0.170	0.10	1.5	26.810	–0.129
40	11	30	41	11	31	107 945.72	–0.029	0.10	–0.2	90.256	–0.721
40	11	29	41	11	30	107 945.72	–0.029	0.10	–0.2	90.256	–0.721
40	13	28	41	13	29	107 995.32	–0.094	0.10	–0.8	143.456	–1.436
40	13	27	41	13	28	107 995.32	–0.094	0.10	–0.8	143.456	–1.436
40	15	26	41	15	27	108 055.13	0.113	0.10	1.0	205.268	–2.523
40	15	25	41	15	26	108 055.13	0.113	0.10	1.0	205.268	–2.523
40	17	24	41	17	25	108 123.93	0.077	0.15	0.5	275.577	–4.098
40	17	23	41	17	24	108 123.93	0.077	0.15	0.5	275.577	–4.098
41	6	36	42	6	37	110 512.31	0.087	0.15	0.5	–6.854	0.076
41	6	35	42	6	36	110 512.31	0.084	0.15	0.5	–6.854	0.076
41	11	31	42	11	32	110 576.88	–0.051	0.10	–0.4	90.190	–0.732
41	11	30	42	11	31	110 576.88	–0.051	0.10	–0.4	90.190	–0.732
41	12	30	42	12	31	110 601.18	0.251	0.10	2.2	116.327	–1.061
41	12	29	42	12	30	110 601.18	0.251	0.10	2.2	116.327	–1.061
41	13	29	42	13	30	110 627.56	–0.064	0.10	–0.6	144.683	–1.471
41	13	28	42	13	29	110 627.56	–0.064	0.10	–0.6	144.683	–1.471
41	15	27	42	15	28	110 688.77	0.208	0.15	1.2	207.996	–2.591
41	15	26	42	15	27	110 688.77	0.208	0.15	1.2	207.996	–2.591

Table 6. continued.

Watson *S*-reduction

Total number of transitions: 342

Transition						Obs. frequency	Obs. – calc.	Weight	*t*	Distortion corrections	
										total	higher
42	9	34	43	9	35	113 168.59	0.111	0.10	1.0	43.307	–0.266
42	9	33	43	9	34	113 168.59	0.111	0.10	1.0	43.307	–0.266
42	10	33	43	10	34	113 186.55	0.001	0.10	0.0	65.487	–0.474
42	10	32	43	10	33	113 186.55	0.001	0.10	0.0	65.487	–0.474
42	11	32	43	11	33	113 207.96	–0.035	0.10	–0.3	89.961	–0.742
42	11	31	43	11	32	113 207.96	–0.035	0.10	–0.3	89.961	–0.742
42	12	31	43	12	32	113 232.63	0.174	0.10	1.5	116.718	–1.081
42	12	30	43	12	31	113 232.63	0.174	0.10	1.5	116.718	–1.081
42	13	30	43	13	31	113 259.61	–0.092	0.10	–0.8	145.746	–1.504
42	13	29	43	13	30	113 259.61	–0.092	0.10	–0.8	145.746	–1.504
42	14	29	43	14	30	113 289.55	–0.026	0.15	–0.1	177.032	–2.025
42	14	28	43	14	29	113 289.55	–0.026	0.15	–0.1	177.032	–2.025
42	15	28	43	15	29	113 321.90	–0.067	0.10	–0.6	210.561	–2.658
42	15	27	43	15	28	113 321.90	–0.067	0.10	–0.6	210.561	–2.658
43	9	35	44	9	36	115 798.80	–0.051	0.10	–0.5	41.831	–0.258
43	9	34	44	9	35	115 798.80	–0.051	0.10	–0.5	41.831	–0.258
43	10	34	44	10	35	115 816.90	–0.242	0.15	–1.4	64.525	–0.473
43	10	33	44	10	34	115 816.90	–0.242	0.15	–1.4	64.525	–0.473
43	11	33	44	11	34	115 839.00	0.061	0.10	0.5	89.566	–0.750
43	11	32	44	11	33	115 839.00	0.061	0.10	0.5	89.566	–0.750
43	12	32	44	12	33	115 863.80	–0.056	0.10	–0.5	116.943	–1.100
43	12	31	44	12	32	115 863.80	–0.056	0.10	–0.5	116.943	–1.100
43	13	31	44	13	32	115 891.50	–0.146	0.10	–1.3	146.643	–1.537
43	13	30	44	13	31	115 891.50	–0.146	0.10	–1.3	146.643	–1.537
43	14	30	44	14	31	115 921.90	–0.244	0.10	–2.2	178.653	–2.073
43	14	29	44	14	30	115 921.90	–0.244	0.10	–2.2	178.653	–2.073
43	15	29	44	15	30	115 955.30	0.070	0.10	0.6	212.957	–2.725
43	15	28	44	15	29	115 955.30	0.070	0.10	0.6	212.957	–2.725

rms deviation: 1.1597

Rotational constants (MHz) and kappa:

	21750	1344.8187	1285.4798	–0.994201
+–	21	0.0030	0.0029	0.000006

Inertial constants and defect (uÅ^2):

	23.236	375.79717	393.14433	–5.889
+–	0.022	0.00085	0.00089	0.023

Quartic distortion constants:

	0.162867	–13.6967	0	0	0
+–	0.00068	0.0090	fixed	fixed	fixed

Standard distortion constants (kHz):

	54.13540	–0.651467	–0.651467	26.74197	–0.651467	26.74197

Sextic and higher distortion constants:

	0.0002868	–0.008587	–0.5276	fixed	fixed
+–	0.00020	0.0032	0.039	fixed	fixed
+–	fixed	fixed			

Significant Digits and Correlation Matrix:

5	0.206	–0.283	–0.391	0.142	–0.116	–0.325	0.286
	8	–0.889	0.167	0.179	0.109	0.089	0.062
		8	0.135	0.031	0.084	0.063	–0.019
			6	–0.312	0.849	0.074	–0.267
				6	–0.384	0.289	0.559
					4	–0.427	0.060
						4	–0.593
							4

Table 7. Spectroscopic constants of $C_2H_5C{\equiv}C{-}C{\equiv}N$.

Parameter	Experimental	Theory
A (MHz)	21750(21)	21878.28
B(MHz)	1344.8187(30)	1338.41
C(MHz)	1285.4798(29)	1281.19
Δ(amu Å^2)	–5.889(23)	–6.22
D_J(kHz)	0.16287(68)	0.14348
D_{JK}(kHz)	–13.6967(90)	–12.6100
H_J(Hz)	0.00029(20)	0.00015
H_{JK}(Hz)	–0.0086(32)	–0.1359
H_{KJ}(Hz)	–0.528(39)	14.30
rms	1.1597	
N	342	

Notes. The spectroscopic constants are in the S-reduction form. The uncertainties represent one standard deviation. rms is the root-mean-square deviation defined by $\mathrm{rms}^2 = \Sigma[(\nu_{\mathrm{obs}} - \nu_{\mathrm{calc}})/u]^2/(N - P)$, where ν_{obs} and ν_{calc} are the observed and calculated frequencies, u is the uncertainty of the observed frequency, N is the number of transitions used in the least-squares fit, and P is the number spectroscopic constants used in the fit. The theoretical rotational constants were obtained in the CCSD/cc-pVTZ calculations and the centrifugal distortion constants were obtained in the B3LYP/cc-pVTZ calculations. Δ is defined by $\Delta = I_c - I_a - I_b$.

Table 8. Spectroscopic constants of Stark coefficients and dipole moment of $C_2H_5C{\equiv}C{-}C{\equiv}N$.

		Stark coefficients $\Delta E^{-2}/(10^{-6}$ MHz V$^{-2})$ cm^2	
Transitions	$\lvert M\rvert$	obs	calc
$5_{1,4} \leftarrow 4_{1,3}$	1	–31.90(50)	–31.963
$6_{0,6} \leftarrow 5_{0,5}$	0	–9.06(10)	–8.975
$6_{0,6} \leftarrow 5_{0,5}$	1	–7.65(20)	–7.606
$6_{0,6} \leftarrow 5_{0,5}$	2	–3.74(20)	–3.516
$6_{1,6} \leftarrow 5_{1,5}$	1	6.99(15)	6.926
$6_{1,5} \leftarrow 5_{1,4}$	1	–11.50(10)	–11.810
$7_{0,7} \leftarrow 6_{0,6}$	0	–10.30(40)	–10.603
$7_{1,7} \leftarrow 6_{1,6}$	0	–21.70(15)	–21.722
$7_{1,7} \leftarrow 6_{1,6}$	1	–18.90(20)	–18.673
$7_{1,7} \leftarrow 6_{1,6}$	2	–9.31(30)	–9.464
Dipole moment			
$\mu_a = 5.713(28)$ $\mu_b = 0.659(3)$ $\mu_c = 0$ $\mu_{\mathrm{TOT}} = 5.751(28)D$			

Notes. Uncertainties represent one standard deviation. μ_c preset at zero.

Acknowledgements. We are grateful to Anne Horn for her skillful assistance. S.C. and J.-C.G. acknowledge the "Programme de Physique et Chimie du Milieu Interstellaire" and the "Programme National de Planétologie" (PCMI and PNP INSU-CNRS) and J.-C.G. acknowledge the "Centre Nationale d'Études Spatiales" (CNES) for financial support. This work has been supported by the Research Council of Norway through a Centre of Excellence Grant (Grant No. 179568/V30). It has also received support from the Norwegian Supercomputing Program (NOTUR) through a grant of computer time (Grant No. NN4654K).

References

Allen, M., & Knapp, G. R. 1978, ApJ, 225, 843
Anicich, V. G. 2003, JPL-Publication
Avery, L. W., Broten, N. W., Macleod, J. M., Oka, T., & Kroto, H. W. 1976, ApJ, 205, L173
Becke, A. D. 1988, Phys. Rev. A, 38, 3098
Bell, M. B., Feldman, P. A., Travers, M. J., et al. 1997, ApJ, 483, L61
Belloche, A., Garrod, R. T., Muller, H. S. P., et al. 2009, A&A, 499, 215
Brandsma, L., & Verkruijsse, H. D. 1981, Studies in Organic Chemistry, Synthesis of acetylenes, allenes, and cumulenes: a laboratory manual (Amsterdam, New York: Elsevier Scientific Pub. Co.), 8, 62
Broten, N. W., Macleod, J. M., Oka, T., et al. 1976, ApJ, 209, L143
Broten, N. W., Oka, T., Avery, L. W., MacLeod, J. M., & Kroto, H. W. 1978, ApJ, 223, L105
Broten, N. W., Macleod, J. M., Avery, L. W., et al. 1984, ApJ, 276, L25
Brown, R. D., Crofts, J. G., Godfrey, P. D., et al. 1975, ApJ, 197, L29
Churchwell, E., & Winnewisser, G. 1975, A&A, 45, 229
Coleman, G. H., Leeper, R. W., & Schulze, C. C. 1946, Inorg. Synth., 2, 90
Crutcher, R., Troland, T., Lazareff, B., Paubert, G., & Kazes, I. 1999, ApJ, 514, L121
Frisch, M. J., Trucks, G. W., Schlegel, H. B., et al. 2009, Gaussian09 (Wallingford, CT: Gaussian, INC.)
Getty, R. R., Kerr, J. A., & Trotman-Dickenson, A. F. 1967, J. Chem. Soc. A, 0, 979
Golden, S., & Wilson, E. B. 1948, J. Chem. Phys., 16, 669
Gordy, W., & Cook, R. L. 1984, Microwave Molecular Spectra, ed. J. W. Sons, XVII (New York)
Guelin, M., & Thaddeus, P. 1977, ApJ, 212, L81
Hakobian, N. S., & Crutcher, R. M. 2011, ApJ, 733
Hollis, J. M., Lovas, F. J., Remijan, A. J., et al. 2006, ApJ, 643, L25
Irvine, W. M. 1987, in Astrochemistry, eds. M. S. Vardya, & S. P. Tarafdar, IAU Symp., 120, 245
Jamal, A., & Mebel, A. 2013, J. Phys. Chem. A, 117, 741
James, D. G. L., & MacCallum, D. 1965, Can. J. Chem., 43, 633
James, D. G. L., & Ogawa, T. 1965, Can. J. Chem., 43, 640
Johnson, D. R., Lovas, F. J., Gottlieb, C. A., et al. 1977, ApJ, 218, 370
Klippenstein, S. J., Georgievskii, Y., & Harding, L. B. 2006, Phys. Chem. Chem. Phys., 8, 1133
Kroto, H. W., Kirby, C., Walton, D. R. M., et al. 1978, ApJ, 219, L133
Landsberg, B., & Suenram, R. 1983, J. Mol. Spectrosc., 98, 210
Lee, C. T., Yang, W. T., & Parr, R. G. 1988, Phys. Rev. B, 37, 785
Leonov, A., Marstokk, K.-M., de Meijere, A., & Møllendal, H. 2000, J. Phys. Chem. A, 104, 4421
Little, L. T., Macdonald, G. H., Riley, P. W., & Matheson, D. N. 1978, MNRAS, 183, 45
Marstokk, K.-M., & Møllendal, H. 1969, J. Mol. Spectr., 4, 470
McKean, D., Craig, N., & Law, M. 2008, J. Phys. Chem. A, 112, 6760
Møllendal, H., Leonov, A., & de Meijere, A. 2005, J. Phys. Chem. A, 109, 6344
Møllendal, H., Cole, G. C., & Guillemin, J. C. 2006, J. Phys. Chem. A, 110, 921
Moureu, C., & Bongrand, J. C. 1920, Ann. Chim. (Fr), 14, 47
Nist web book, w. s. accessed January 2013, http://webbook.nist.gov/chemistry/
Opendak, M. G., & Varshalovich, D. A. 1986, Soviet Astron., 30, 274
Peterson, K. A., & Dunning, T. H. 2002, J. Chem. Phys., 117, 10548
Purvis, G. D., & Bartlett, R. J. 1982, J. Chem. Phys., 76, 1910
Ray, B. S. 1932, Z. Phys., 78, 74
Rudic, S., Murray, C., Harvey, J. N., & Orr-Ewing, A. J. 2004, J. Chem. Phys., 120, 186
Scuseria, G. E., Janssen, C. L., & Schaefer, H. F. 1988, J. Chem. Phys., 89, 7382
Snyder, L. E., & Buhl, D. 1971, ApJ, 163, L47
Snyder, L. E., Hollis, J. M., Jewell, P. R., Lovas, F. J., & Remijan, A. 2006, ApJ, 647, 412, part 1
Solomon, P. 1973, Phys. Today, 26, 32
Solomon, P. M., Jefferts, K. B., Penzias, A. A., & Wilson, R. W. 1971, ApJ, 168, L107
Sørensen, G. O. 1967, J. Mol. Spectr., 22, 325
Strubing, D., Neumann, H., Klaus, S., Hubner, S., & Beller, M. 2005, Tetrahedron, 61, 11333
Troe, J. 2003, Chem. Rev., 103, 4565
Turner, B. E. 1971, ApJ, 163, L35
Van der Welle, R. A., & Brandsma, L. 1973, Rec. Trav. Chim. Pays-Bas, 92, 667
Vasyunin, A. I., & Herbst, E. 2013, ApJ, 769, 34
Watson, J. 1977, Vibrational Spectra and Structure., ed. J. Durig (Amsterdam: Elsevier), 8, 1
Winnewisser, G., & Walmsley, C. M. 1978, A&A, 70, L37
Wodarczyk, F., & Wilson, E. B. 1971, J. Mol. Spectr., 37, 445
Woon, D. E., & Herbst, E. 2009, ApJS, 185, 273